Aust. J. Phys., 1988, **41**, 393–402

Concerning Single Crystal Reflectivity Curves*

A. McL. Mathieson

Chemistry Department, La Trobe University,
Bundoora, Vic. 3083, Australia.

Abstract

The extinguished reflectivity curve of a Bragg single crystal reflection represents the basic experimental evidence for the determination of accurate structure factors. In normal measurement procedures of one-dimensional (1D) 'counter' profiles, information on such curves is obscured by the presence of other, more dominant components. It is therefore difficult to separate out these curves so that a realistic correction for extinction can be applied. By considering the 'shape' of a Bragg reflection in the plane of diffraction from the $\Delta\omega$, $\Delta 2\theta$ viewpoint, procedures have been deduced for practical zero wavelength dispersion measurement of reflectivity curves for virtually any θ value and, with these curves, corrections can be applied to produce extinction-free structure factor values. Attention is drawn to the fact that the width of the experimental reflectivity curve (say at half maximum) can provide a valuable criterion to assist in attaining the 'kinematical limit'.

1. Introduction

'Imperfect' crystals constitute the majority of single crystals obtained in Nature or from chemical syntheses. It is therefore for this class that the majority of diffraction studies continue to be applied and, since dynamical procedures involving fringe measurement are not useable on such specimens, it is for this class that there is a need to derive structure factor values by measurement of intensity distribution diffracted by single crystal reflections. Despite this situation, exploration of the nature of Bragg reflections in more than one dimension to learn about the components which contribute to the intensity distribution of the reflection has received relatively limited attention. This is despite the increased potential for such investigations offered by position-sensitive detectors (PSD). So far, such detectors have been used simply to collect more data, more rapidly, from more specimens.

The exploration of the subject of imperfect crystals initiated by Darwin, Bragg and colleagues (e.g. Darwin 1922; Bragg *et al.* 1921*a*, 1921*b*, 1926) has not really changed greatly in respect of experimental measurement. The focus has been on the estimation of integrated intensity—which necessarily includes all the components of the experimental set-up. Although it was realised by Robinson (1933) that one should determine the reflectivity curve and apply point-by-point corrections to derive an extinction-free result (see Fig. 1), it was not fully appreciated how much the true intrinsic reflectivity curve was smeared out and obscured by the other components.

* Paper presented at the International Symposium on Accuracy in Structure Factor Measurement, held at Warburton, Australia, 23–26 August 1987.

0004-9506/88/030393$03.00

It is only relatively recently that there has been more concern with determining this primary evidence, stimulated in particular by the work with γ-rays (see e.g. Schneider 1976).

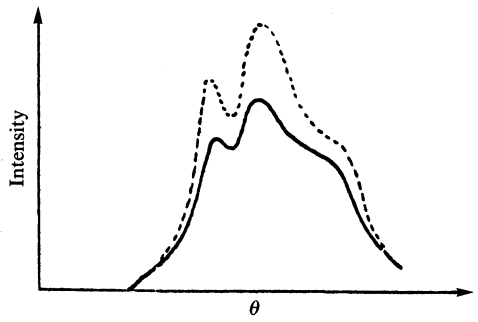

Fig. 1. Representation of a measured reflectivity curve (full) and its equivalent, corrected for extinction (dashed curve). [From Robinson (1933).]

An important aspect of dealing with reflectivity curves is to arrive at experimental estimates of structure factors without undue dependence on theoretical estimates. This approach is needed to authenticate unexpected deformation density results, such as those of Dunitz and coworkers (e.g. Dunitz and Seiler 1983; Dunitz *et al.* 1983). Theoretical estimates of structure factors are inevitably based on certain assumptions concerning bonding electron density and so, because of this dependence, we can find ourselves unable to sort out the physical realities.

2. Relevance of Dealing in $\Delta\omega$, $\Delta 2\theta$ Space

Generally, measurements are carried out not on one but many Bragg reflections distributed throughout diffraction space and it is necessary to treat these on a consistent basis. To navigate from one reflection to another, we use the concept of reciprocal space. However, when we dock onto a specific reflection, our aim is to carry out measurements of the intensity distribution around this reflection in such a way that we can make as direct a comparison as possible with the measurements on the other reflections and hence extract the information relevant to an accurate estimate of a structure factor.

The intensity distribution of a Bragg reflection arises from the convolution of the distributions of the various components which contribute—(say) source, the dispersions of the monochromator crystal (if included) and of the specimen crystal, the mosaic spreads of these two crystals, the distances between source/monochromator, crystal/detector, etc. For consistency from reflection to reflection, we need to use exactly the same limits for each component and we wish to extract the reflectivity curve but, in general, exclude the supernumerary information in the other components.

For such measurements, there is a problem in dealing in reciprocal space, in that most of the components alter in scale as one moves further from the origin of reciprocal space. If, however, we deal in angular $\Delta\omega$, $\Delta 2\theta$ space then, for most components, it is unnecessary to apply a scale factor to facilitate comparison. It is instructive to compare (i) a low-angle and (ii) a high-angle reflection in reciprocal space and in $\Delta\omega$, $\Delta 2\theta$ space, as in Fig. 2. In reciprocal space (Figs 2*a* and 2*b*), the dimensions of the components all change with θ, being proportional to d^* with a $\tan\theta$ scale expansion for the wavelength band component. In addition, the relative

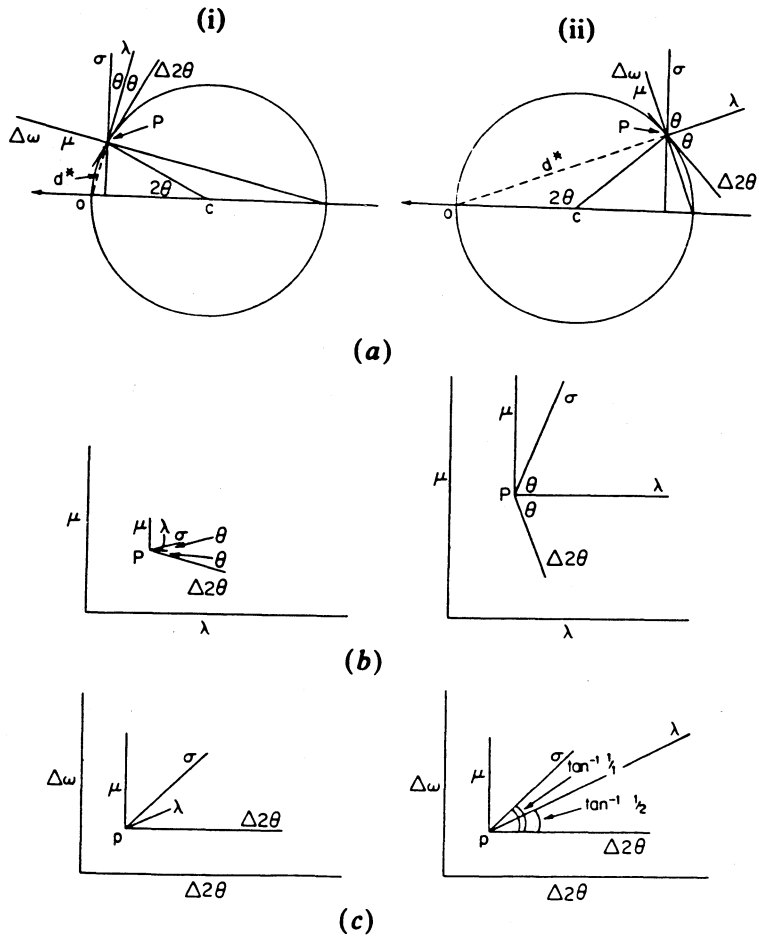

Fig. 2. Comparison of (i) low-θ and (ii) high-θ reflections: (*a*) Ewald-circle construction for diffraction at a point P associated with a vector d^* in reciprocal space. The angular variables $\Delta\omega$, $\Delta 2\theta$ and the components μ, σ, λ are identified. (*b*) Enlarged scale diagrams of the details around points P in (*a*) showing how, in reciprocal space, the components μ, σ, λ change both their size and mutual disposition with a change in θ. (*c*) Relationships between the components μ, σ, λ and the angular variables in $\Delta\omega$, $\Delta 2\theta$ space. The invariance of the mutual disposition of the components μ, σ, λ and the angular variables $\Delta\omega$, $\Delta 2\theta$ is demonstrated as is the dimensionality of the components μ, σ. The only component varying intrinsically with θ is λ, whose length is proportional to $\tan\theta$.

dispositions of the component loci change with θ. By contrast, when we view the local diffraction space adjacent to the Bragg reflection in terms of angular measure $\Delta\omega$, $\Delta 2\theta$ (Fig. 2*c*), then the mosaic spread of the specimen crystal, the source distribution and the measurement across the detector $\Delta 2\theta$ do not change with θ, nor does the relative disposition of the loci of these components. Only one item changes systematically with θ, namely that of the wavelength band and that is in a well-established way.

So, for ease of comparison of reflections at different scattering angles, *and* for ease of detection of minor differences between them, there are obvious advantages in dealing

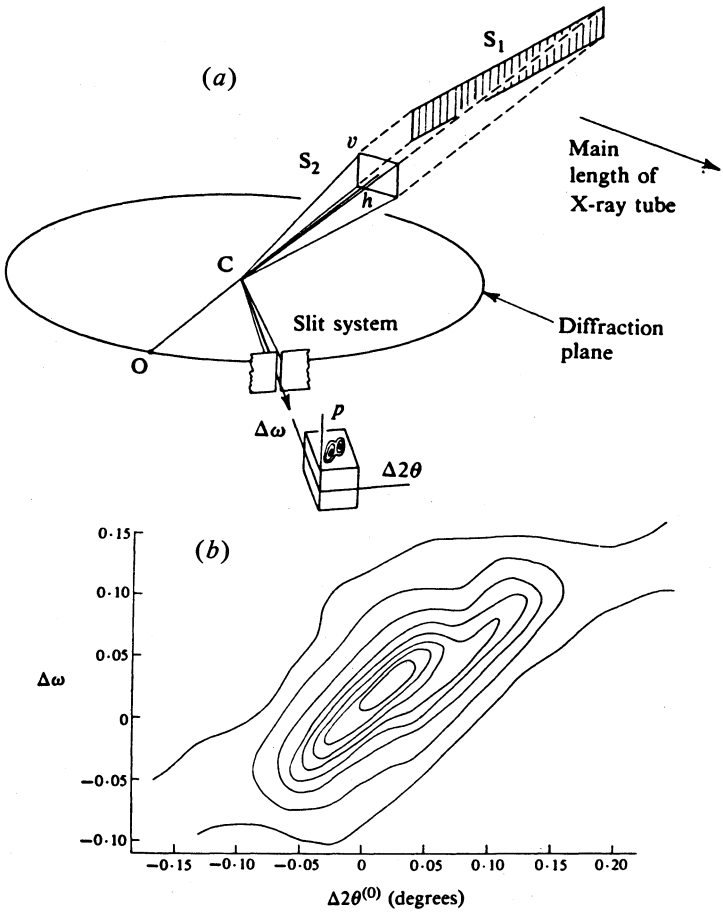

Fig. 3. (*a*) Conventional experimental arrangement with the main length of the X-ray source S_1 in the plane of diffraction and where S_2, of width h and height v, corresponds to the effective source as seen by the specimen crystal C. The aperture system in front of the (scintillation) detector is narrow in the diffraction plane and elongated perpendicular to it. The intensity distribution $I(\Delta\omega, \Delta 2\theta)$ of a Bragg reflection with local reference axes $\Delta\omega$, $\Delta 2\theta$, p is indicated in relation to the diffractometer plane. (*b*) The corresponding measured intensity distribution projected down p.

in terms of local angular measure—the specimen local angular movement $\Delta\omega$ and the detector angular dimension $\Delta 2\theta$. With the resultant 2D array of measurements (data points), one can carry out appropriate affine transformations (Mathieson and Stevenson 1985) so that components can be more readily recognised, appreciated and measured.

3. Intrinsic Reflectivity Curve

Most of the components involved in determining the shape of a Bragg reflection are there only to supply measurable intensity and, in a sense, need to be discarded

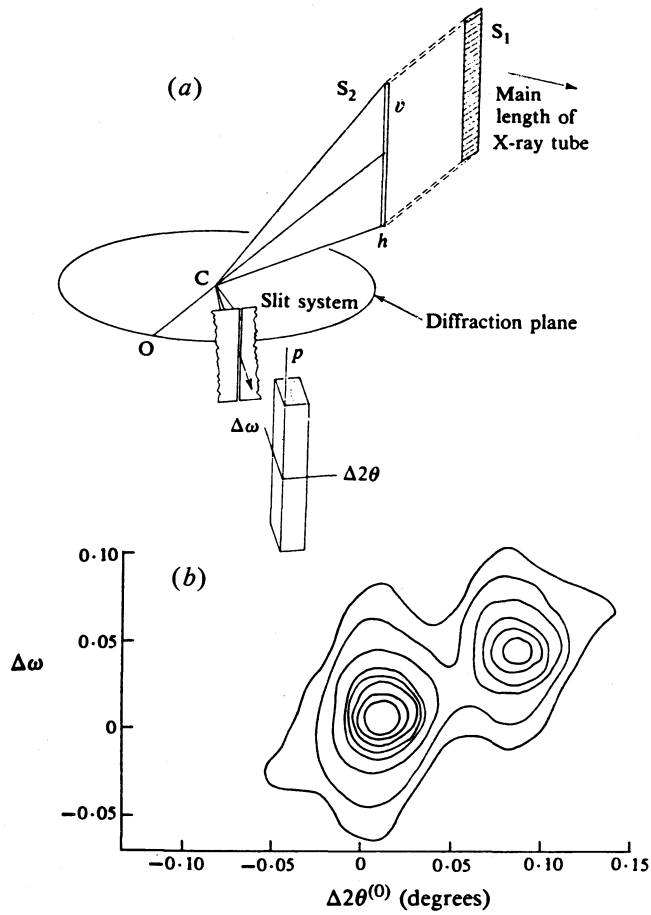

Fig. 4. (*a*) Experimental arrangement with the main length of the X-ray source S_1 perpendicular to the plane of diffraction and where S_2, of width h and height v, corresponds to the effective source as seen by the specimen crystal C. The aperture system in front of the detector is narrow in the diffraction plane and sufficiently elongated perpendicular to it to collect the total height of the signal. The intensity distribution $I(\Delta\omega, \Delta 2\theta, p)$ of a Bragg reflection, with local reference axes $\Delta\omega, \Delta 2\theta, p$, is indicated in relation to the diffraction plane. (*b*) The corresponding measured intensity distribution projected down p.

or, at least, have their effect minimised in order to extract the essential information contained in the experimental reflectivity curve. However, we must be able to establish and use the same truncation limits for all components of all reflections if we are to achieve exactly comparable estimates for all reflections. Again, from this viewpoint, dealing in $\Delta\omega$, $\Delta 2\theta$ space is advantageous.

Ideally, we should aim for measurement procedures where we can recognise the wavelength component and separate it from the reflectivity curve or devise procedures where the wavelength dispersion makes zero contribution.

4. Zero Wavelength Dispersion

In classical terms, only one procedure is available to provide a measured reflectivity curve which is essentially free of the wavelength component (see Compton and Allison 1935). With a two-crystal system (first crystal M and second C), where the rotation axes of the two crystals are parallel and the measurements are carried out in the so-called 'parallel' configuration, the 'counter' profile measurement of the second crystal yields its reflectivity curve. The zero wavelength dispersion (ZWD) reflectivity curve can only be determined for one Bragg reflection, i.e. when $\theta_C = \theta_M$. Away from that setting, the wavelength dispersion component makes a contribution which convolutes with the reflectivity curve. So the classical procedure is highly selective and severely limited in its application.

To explore whether there are alternative and more general approaches, let us consider measurements on a small single crystal in $\Delta\omega$, $\Delta 2\theta$ space. One particular problem is that, under normal circumstances, we are involved with too many components. Some, of no great relevance to our purpose, make too gross a contribution and swamp the reflectivity curve, even in the 2D presentation. As shown in Fig. 3*a*, we have a standard squarish source which dominates the overall distribution of Fig. 3*b*, so that it is difficult to extract sufficiently detailed information on the mosaic distribution μ (= reflectivity curve) and the wavelength distribution λ.

If, however, we use a different source, 'tall and narrow', as in Fig. 4*a*, its angular contribution in the diffraction plane is small but its out-of-plane shape matches that of the detector aperture so, overall, measurable intensity is not lost. With this set-up, the effective source component is much reduced in its dimension (Fig. 4*b*). Also, since there are only two dominant functions in this 2D presentation, μ and λ, one can readily sort out one from the other. We are mainly interested in the μ distribution, but can utilise the λ distribution to check on the general smearing effect by comparing with the known distribution for the characteristic or selected wavelength band (in the case of synchrotron radiation). Since the source distribution is small relative to the reflectivity curve, it can be removed by deconvolution.*

The measurement procedure detailed above (see Mathieson and Stevenson 1984) does, of course, require 2D data collection from which one can extract information concerning μ and λ. The reflectivity curve is intrinsically 1D for any one reflection in a certain orientation about its pole so one may ask whether, using the $\Delta\omega$, $\Delta 2\theta$ viewpoint, one can arrive at an essentially 1D procedure which would have ZWD across the full range of θ.

We consider the 'film' 1D profile

$$I(\Delta 2\theta^{(2)}) = \int_{\Delta\omega_1}^{\Delta\omega_2} I(\Delta\omega,\ \Delta 2\theta^{(2)})\, \mathrm{d}(\Delta\omega), \tag{1}$$

which involves integration parallel to $\Delta\omega$ while operating in the $\omega/2\theta$ scan mode (Mathieson and Stevenson 1986*a*). Fig. 5 shows (*a*) a low-angle and (*b*) a high-angle case using synthetic distributions for the individual components. The $\Delta\omega$, $\Delta 2\theta^{(2)}$ distributions are shown and the 'film' profiles corresponding to integration vertically

* One may note that the combination of a tall and narrow source and a small crystal can have angular divergence which, for appropriate distances, is comparable with that available from a synchrotron source.

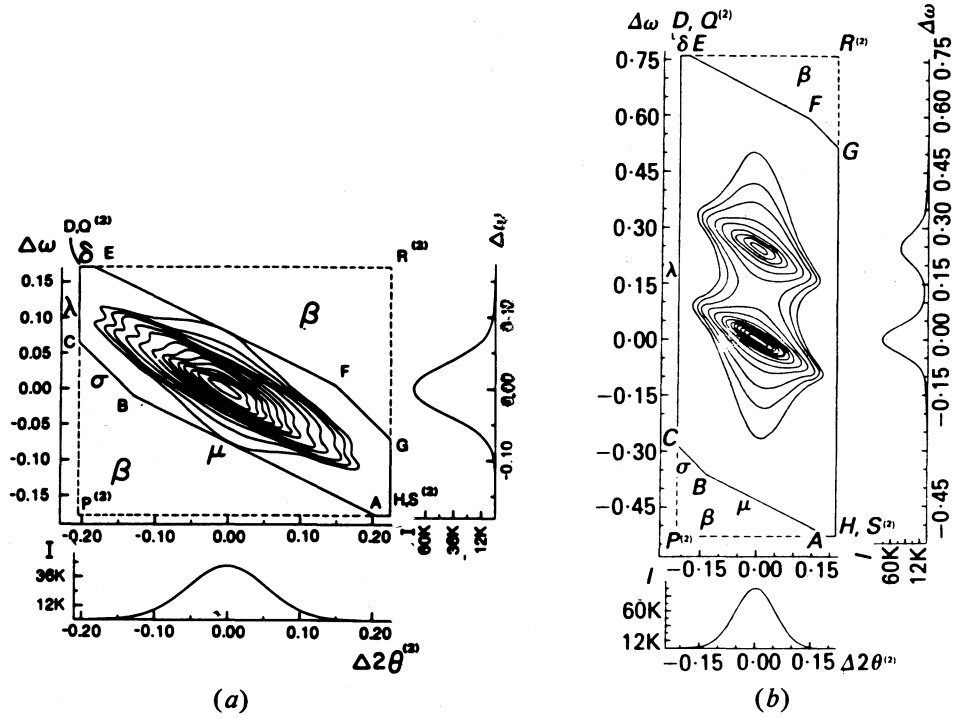

Fig. 5. Synthetic distributions presented in the $\omega/2\theta$ scan mode, i.e. $I(\Delta\omega, \Delta 2\theta^{(2)})$, for (*a*) low-angle reflection and (*b*) a high-angle reflection with the resultant 1D 'film' profile below the respective 2D distribution. [Note that (*b*) is half the scale of (*a*).]

appear below the respective 2D distributions. The 1D 'film' profiles do not involve the λ component, and hence are ZWD. They are directly comparable without scalar change despite the gross change in angular dispersion of the wavelength component, which is about 10:1 in the case shown. This procedure is applicable, using the $\omega/2\theta$ scan mode, for non-monochromator and monochromator situations and has no restrictions in respect of θ. Its suitability for PSD application is evident.

The second possible procedure which can be derived from examination of the situation in $\Delta\omega$, $\Delta 2\theta$ space relates to the following 'counter' 1D profile (note that in a non-monochromator case, there is no means of eliminating the λ dispersion from the 'counter' profile for general θ):

$$I(\Delta\omega) = \int_{\Delta 2\theta_1^{(0)}}^{\Delta 2\theta_2^{(0)}} I(\Delta\omega,\ \Delta 2\theta^{(0)})\, \mathrm{d}(\Delta 2\theta^{(0)}). \tag{2}$$

This is applicable, as in the classical case, only to a two-crystal situation, i.e. involving a monochromator crystal and a small specimen crystal. However, it does involve additional complexity over the classical situation, in that it requires the flexibility of a five-circle system since the specimen crystal four-circle diffractometer must be capable of rotating in a cradle about the beam diffracted from the monochromator crystal.

With this arrangement, which has been treated in detail elsewhere (see Mathieson 1987), it is possible to carry out a ZWD measurement over the range from $\theta_C = 0$ to θ_M. It thus expands the capability of the classical procedure. In this arrangement, use of a high θ_M monochromator would be advantageous.

5. 'Kinematical Limit'

The procedures outlined above can yield measures of extinguished reflectivity curves after deconvolution to allow for the source component. We should note that, although monochromated synchrotron sources do have a small wavelength band, its contributions cannot simply be ignored (Mathieson 1988) and use of a ZWD procedure or appropriate correction for the λ component is advisable.

When one obtains a well-defined ZWD reflectivity curve for a single reflection, one can use power-transfer relationships as a first approximation to apply point-by-point corrections (cf. Schneider 1977; Mackenzie and Mathieson 1979). With this approach, one has no absolute check as to how far the corrected curve has to be raised to attain the zero-extinction limit. When one obtains reflectivity curves for a set of Bragg reflections, then one is in a rather more powerful position in that the correction for a given reflectivity should be applicable to all reflections, i.e. a universal correction procedure is used for that particular set-up. However, we have no criterion to check whether the correction used is adequate, too small or too large.

Let us remind ourselves of the situation in 1926. Bragg *et al.* (1926), in dealing with the 'kinematical limit', observed that it represented an *upper limit* of integrated intensity. The difficulty was that they had no guideline to establish how far the measured extinguished value for a given reflection lay below the limit, nor how far it had to be lifted to reach the upper limit for that reflection. So, it was at that point, regrettably, that they proposed reliance on the theoretical structure factors to establish how far below the limit they were. By implication they assumed (and it may have been true then) that the theoretical values, crude as they were at that time, were more significant, i.e. more accurate, than the experimental values. We have tended to follow this lead for some 60 years. The basic problem, then and for long afterwards, was that there was no other test—except for very limited measurements on reflectivity curves of rather scarce 'perfect' crystals.

We can now see that if we turn from integrated intensity—which in terms of measurement is zero-dimensional although formally it has the dimension of angle—to the reflectivity curve, we obtain valuable additional information in terms of its shape and we can use this extra information. The point is that the 'shape' of the reflectivity curve is differentially modified by the operation of extinction; it becomes *wider* at (say) the half maximum level. So, here we have an experimental criterion concerning the 'kinematical limit' whose trend is *opposite* to that of the extinguished integrated intensity. In other words, this provides a criterion which has a defined *lower limit* as one moves to zero reflectivity.

Each point in a reflectivity curve is extinguished and has to be corrected upwards; however, only so that the width of the reflection at half maximum does not go beyond the limit set by the weak reflections. We can illustrate this point with some recent results by Schulz and coworkers (Höche *et al.* 1986), where the data on width at half maximum were collected on the synchrotron DESY. Fig. 6*a* shows the results for a CaF_2 crystal of size 90 μm at $\lambda = 1{\cdot}714$ Å. The more intense reflections are

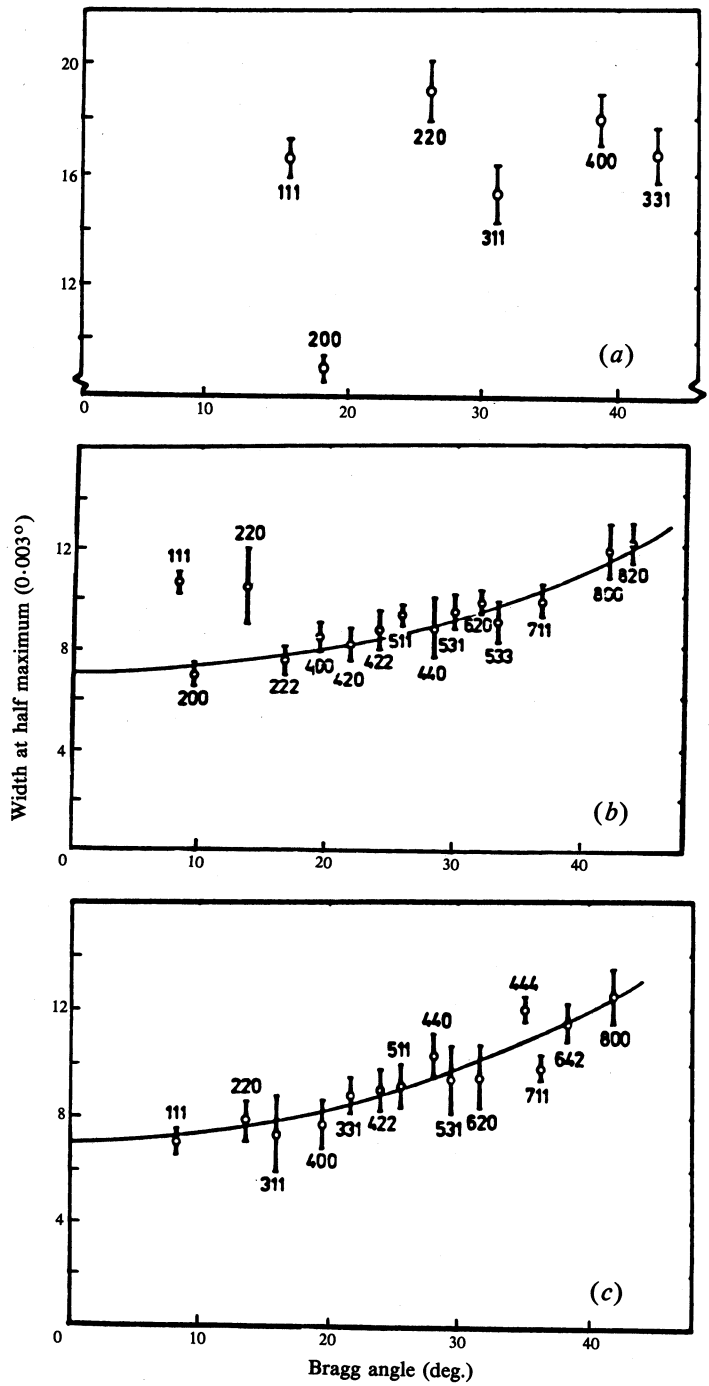

Fig. 6. Measured values of width at half maximum (*a*) for a 90 μm CaF_2 crystal at λ = 1·714 Å, (*b*) for the 90 μm CaF_2 crystal at λ = 0·917 Å and (*c*) for a 6 μm CaF_2 crystal at λ = 0·917 Å. Note that for (*c*) the experimental set-up from which these results were derived involved 'crossed' crystals and so differed from the set-up relating to (*a*) and (*b*).

significantly wider. When the wavelength is reduced to 0·917 Å (Fig. 6*b*), the values fall more closely together with the more intense reflections still high. With a 6 μm crystal (Fig. 6*c*), the differences are much reduced. Even so, I would conjecture that close inspection of the shapes of individual reflections, rather than averaging equivalents, might yield significant differences.*

It is evident that, to establish reflectivity curves of sufficient precision to use for this purpose, angular displacements will need to be established to the order of 0·001° or even 0·0005°. Given that such reflectivity curves can be obtained, corrected, and tested against width at half maximum, then there seems every reason to expect that we can indeed achieve for X-rays of conventional wavelengths what Darwin hoped for in the early 1920s and what Robinson sought to achieve in 1933.

References

Bragg, W. L., Darwin, C. G., and James, R. (1926). *Philos. Mag.* **1**, 897–922.
Bragg, W. L., James, R. W., and Bosanquet, C. H. (1921*a*). *Philos. Mag.* **41**, 309–37.
Bragg, W. L., James, R. W., and Bosanquet, C. H. (1921*b*). *Philos. Mag.* **42**, 1–17.
Compton, A. H., and Allison, S. K. (1935). 'X-rays in Theory and Experiment' (Van Nostrand: New York).
Darwin, C. G. (1922). *Philos. Mag.* **43**, 800–29.
Dunitz, J. D., Schweizer, W. B., Seiler, P., Schluter, A.-R., and Szeimeis, G. (1983). *Helv. Chim. Acta* **66**, 123–33.
Dunitz, J. D., and Seiler, P. (1983). *J. Am. Chem. Soc.* **105**, 7056–8.
Höche, H. R., Schulz, H., Weber, H.-P., Belzner, A., Wolf, A., and Wulf, R. (1986). *Acta Cryst.* A **42**, 106–10.
Mackenzie, J. K., and Mathieson, A.McL. (1979). *Acta Cryst.* A **35**, 45–50.
Mathieson, A.McL. (1987). *Acta Cryst.* A **43**, 552–4.
Mathieson, A.McL. (1988). *Acta Cryst.* A **44** (in press).
Mathieson, A.McL., and Stevenson, A. W. (1984). *Aust. J. Phys.* **37**, 657–65.
Mathieson, A.McL., and Stevenson, A. W. (1985). *Acta Cryst.* A **41**, 290–6.
Mathieson, A.McL., and Stevenson, A. W. (1986*a*). *Acta Cryst.* A **42**, 435–41.
Mathieson, A. McL., and Stevenson, A. W. (1986*b*). *Acta Cryst.* A **42**, 223–30.
Robinson, B. W. (1933). *Proc. R. Soc. London* A **142**, 422–47.
Schneider, J. R. (1976). *J. Appl. Cryst.* **9**, 394–402.
Schneider, J. R. (1977). *Acta Cryst.* A **33**, 235–43.

Manuscript received 21 September, accepted 27 November 1987

* Equivalent reflections need not have identical reflectivity curves, unless the extinction effects are isotropic (see Mathieson and Stevenson 1986*b*). Further, as observed above, even with synchrotron sources, wavelength dispersion makes itself felt.